

**THE EXAMINATION OF THE EFFECT OF  
POLARIZATION ON THE RADIATION LOSSES OF  
BENT OPTICAL FIBERS**

**A THESIS  
SUBMITTED TO THE DEPARTMENT OF ELECTRICAL AND  
ELECTRONICS ENGINEERING  
AND THE INSTITUTE OF ENGINEERING AND SCIENCES  
OF BILKENT UNIVERSITY  
IN PARTIAL FULFILLMENT OF THE REQUIREMENTS  
FOR THE DEGREE OF  
MASTER OF SCIENCE**

**By  
Süleyman Gökhan TANYER**

**July 1990**

TK  
7871.65  
T169  
1990

THE EXAMINATION OF THE EFFECT OF  
POLARIZATION ON THE RADIATION LOSSES OF  
BENT OPTICAL FIBERS

A THESIS

SUBMITTED TO THE DEPARTMENT OF ELECTRICAL AND  
ELECTRONICS ENGINEERING

AND THE INSTITUTE OF ENGINEERING AND SCIENCES  
OF BILKENT UNIVERSITY

IN PARTIAL FULFILLMENT OF THE REQUIREMENTS  
FOR THE DEGREE OF  
MASTER OF SCIENCE

S. Gökhan Tanyer  
tanyer@bilken.edu.tr

By

Süleyman Gökhan Tanyer

July 1990

TK

2871.65

.T169

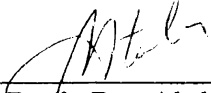
1990

B. 1993

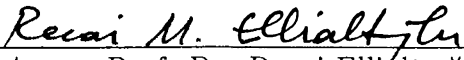
I certify that I have read this thesis and that in my opinion it is fully adequate, in scope and in quality, as a thesis for the degree of Master of Science.

  
\_\_\_\_\_  
Assoc. Prof. Dr. Ayhan Altıntaş (Principal Advisor)

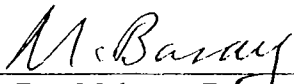
I certify that I have read this thesis and that in my opinion it is fully adequate, in scope and in quality, as a thesis for the degree of Master of Science.

  
\_\_\_\_\_  
Prof. Dr. Abdullah Atalar

I certify that I have read this thesis and that in my opinion it is fully adequate, in scope and in quality, as a thesis for the degree of Master of Science.

  
\_\_\_\_\_  
Assoc. Prof. Dr. Recai Elliältiođlu

Approved for the Institute of Engineering and Sciences:

  
\_\_\_\_\_  
Prof. Dr. Mehmet Baray  
Director of Institute of Engineering and Sciences

To Mom and Dad

## ABSTRACT

### THE EXAMINATION OF THE EFFECT OF POLARIZATION ON THE RADIATION LOSSES OF BENT OPTICAL FIBERS

Süleyman Gökhun Tanyer  
M.S. in Electrical and Electronics Engineering  
Supervisor: Assoc. Prof. Dr. Ayhan Altıntaş  
July 1990

It has long been recognized that the bending losses in weakly guiding optical fibers, is independent of the polarization for large bend radius. We showed this fact using the volume equivalent current method. The procedure is then applied to a helically bent fiber, and it is shown that the radiation from the helical fiber is also independent of the polarization as long as the fiber is weakly guiding.

## ÖZET

### BÜKÜLMÜŞ OPTİK FİBERLERDE POLARİZASYONUN BÜKÜLME KAYIPLARINA ETKİSİNİN İNCELENMESİ

Süleyman Gökhan Tanyer

Elektrik ve Elektronik Mühendisliği Bölümü Yüksek Lisans

Tez Yöneticisi: Doç. Dr. Ayhan Altıntaş

Temmuz 1990

Zayıfça kılavuzlayan optik fiberlerde büyük bükülme yarıçapları için bükülme kayıplarının polarizasyona bağımlı olmadığı uzun zamandır biliniyordu. Bu tez çalışmasında bükülmüş fiberi dielektrik bir anten gibi kabul edip, bu antenden yayılan ışınının kayıp gücü vermesi esasına dayanan eşdeğer akım yöntemi kullanarak bükülmüş fiberin bükülme kaybının polarizasyona bağımlı olmadığı gösterildi. Daha sonra bu yöntem zayıfça kılavuzlayan helezon şeklinde bükülmüş fibere de uygulandı ve aynı sonuca varıldı.

## ACKNOWLEDGEMENT

I would like to express my deep gratitude to Assoc. Prof. Dr. Ayhan Altıntaş for his invaluable guidance and efforts during the development of this study.

I am also deeply indebted to Prof. Dr. Altunkal Hızal, my undergraduate instructor of the courses on microwaves and antennas, who ignited my interest in electromagnetics.



# Contents

<b>1</b>	<b>INTRODUCTION</b>	<b>1</b>
<b>2</b>	<b>VOLUME EQUIVALENT CURRENTS</b>	<b>5</b>
<b>3</b>	<b>ANALYSIS OF DIELECTRIC OPTICAL WAVEGUIDES</b>	<b>9</b>
3.1	FIELDS OF PLANAR WAVEGUIDES . . . . .	9
3.2	FIELDS OF CIRCULAR WAVEGUIDES (FIBERS)	13
3.3	FIELDS OF WEAKLY GUIDING FIBERS	15
<b>4</b>	<b>LOSS IN BENT FIBERS</b>	<b>19</b>
4.1	Perpendicular Polarization Case . . . . .	22
4.2	Parallel Polarization Case	25
<b>5</b>	<b>LOSS IN HELICAL FIBERS</b>	<b>31</b>
<b>6</b>	<b>CONCLUSIONS</b>	<b>37</b>

<i>CONTENTS</i>	vii
<b>A</b> Scalar and vector operators	<b>38</b>
<b>B</b> Bessel functions	<b>39</b>
<b>C</b> Eigenvalue equations for step-profile circular fiber	<b>40</b>

## List of Figures

1.1	The layers of an optical waveguide . . . . .	2
1.2	The refractive index profile of step-profile waveguide . . . . .	2
1.3	The refractive index profile of graded-profile waveguide . . . . .	2
2.1	Coordinate of the source and the field points . . . . .	8
3.1	Section of a step-profile planar waveguide . . . . .	10
3.2	Section of a step-profile circular waveguide . . . . .	13
4.1	The circularly bent fiber . . . . .	23
4.2	Circular fiber, perpendicular polarization case . . . . .	25
4.3	Circular fiber, parallel polarization case . . . . .	26
5.1	Helically bent fiber . . . . .	32

# Chapter 1

## INTRODUCTION

Optical waveguides that are used for communication applications, are made of highly transparent dielectric materials. They are designed to carry electromagnetic energy in the visible or infrared regions of frequency spectrum. Those highly flexible dielectrics have very small loss, and high bandwidth transmission characteristics. For those reasons, they are used for transmission of voice, data, and video signals which requires high information capacity. It is also noted that optical waveguides have the potential for being used wherever twisted wire pairs or coaxial cables are used in a communication system.

Optical waveguides, often called fibers, are generally made up of three coaxial layers as shown in Fig. 1.1. In the center there exists a medium called the *core*, surrounded by a second medium, called the *cladding*. The protective layer *jacket*, covers the cladding medium, and is used for giving mechanical strength to the waveguide. It also protects the inner layers from moisture, and mechanical disturbances. Depending on the application, the refractive index profile in the core may be uniform or non-uniform. The former case is referred to as *step-profile fibers*, and the latter case is *graded-profile fibers*. Figures 1.2, and 1.3 show the refractive index profile of each type of fiber. Since the idea of optical waveguides is to guide the electromagnetic energy along its path, the refractive index of the core region must be greater than the refractive index of the cladding region. So that, most of the propagating energy is captured by the core region, and only a small portion is kept in the cladding region.

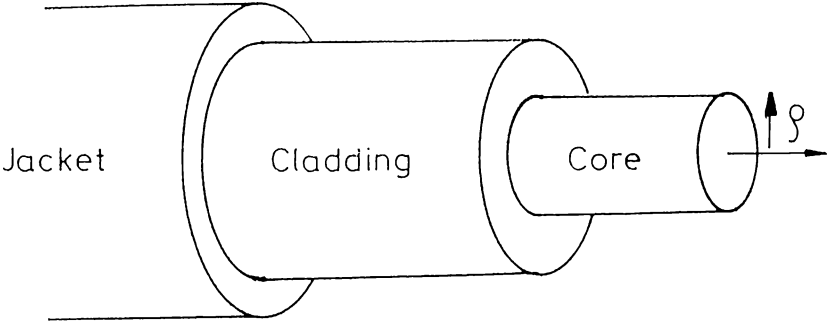


Figure 1.1: The layers of an optical waveguide

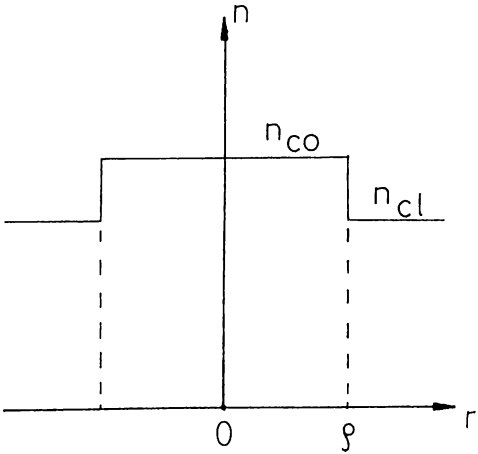


Figure 1.2: The refractive index profile of step-profile waveguide

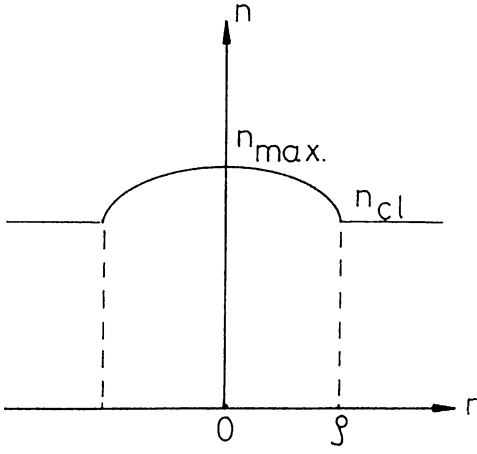


Figure 1.3: The refractive index profile of graded-profile waveguide

An optical waveguide can accommodate one or more propagating modes depending on the refractive index and size of the core and cladding. As the name implies, the *single-mode fiber* carries only one propagating mode at the specified frequency, and *multi-mode fiber* has more than one propagating modes. Multi-mode fibers are mostly used in short distance communication applications, and in fiber sensors. In telecommunication systems, the cladding and the core refractive indices are designed to be very close to each other to limit the dispersion. Those kind of waveguides are called *weakly guiding fibers* to which the analysis in the thesis is restricted.

If we bend a fiber, we observe a radiation loss which is commonly referred to as *Bending Loss*. Since it is an important problem in optical communication systems, considerable amount of work has been done in the analysis of bending losses. We may assume Marcatili's work [1] in 1969 to be the first in this field. He investigated the radiation effects of a dielectric slab using a rigorous method. He had some asymptotic expansions in his solution. Shevchenko [2] generalized the known radiation mechanism for the slab to the case of fiber. Levin [3] solved for the approximate values of the electromagnetic field to reach a bending loss expression. Snyder, White, and Mitchell [4] have derived the bending loss formula for both the slab and the fiber cases. Marcuse [5] analyzed the bending losses of the asymmetric slab waveguide. Chang, and Kuester [6] noted that the results obtained previously, do not always agree and so that there exist very large difference factors. They derived the bending loss formula by solving the approximate values of the fields of bent dielectric slab and fiber. Marcuse [7] derived the bending loss formula by determining the coefficients of a field expansion. Those coefficients are found by matching the field expansion in cylindrical waves to the mode field of the straight fiber. In his work, he assumed the waveguide to be weakly guiding. Later, Marcuse [8] analyzed the radiation loss of a helically deformed optical fiber. He considered only one turn of the helix, and derived the bending loss formula using the same procedure that he has used in his previous work [7]. He has neglected the optical effect of the torsion due to the twist of the fiber [9]. Altıntaş and Love [10] used a relatively simple volume equivalent current method to reach a power attenuation coefficient for helical fibers. They noted that the helical loss could be so high that it acts as an effective cutoff for that mode. In this work the bending loss of a circularly bent fiber for two

orthogonal polarizations is derived, and is proven that the loss is independent of polarization as reported earlier [11]. Also, we have analyzed the helically bent fiber problem, and derived the bending loss formula by including the effect of the torsion due to the twist of fiber [12].

The outline of the thesis is as follows. In Chapter 2, *Volume Equivalent Current Method* is described. In Chapter 3, the analysis of step-profile planar and circular waveguides is given. The weakly guiding waveguide fields are later derived. In Chapter 4, loss in bent optical waveguides is examined using the previously introduced volume equivalent current method. In this analysis, the field of bent fiber is assumed to be equal to the undistorted field of the straight fiber. This approximation is good for small radiation losses. As far as the bending radius is large compared to the core radius, as in most practical bends, this does not bring a serious limitation. Our analysis is done for two perpendicular polarizations to check for the effects of polarization on the radiation loss of a circularly bent fiber. In Chapter 5, the same method is applied to a helically bent optical waveguide. Since torsion is present due to twist of fiber [9], we included that effect in the analysis, and assumed the polarization to have a slip related to the geometrical helix parameters of the fiber. Finally, conclusions are given in Chapter 6.

In the analysis, a sinusoidally-varying time dependence with angular frequency  $\omega$  ( $\exp(j\omega t)$ ) is assumed, and suppressed.

## Chapter 2

### VOLUME EQUIVALENT CURRENTS

The expressions for the electric and magnetic fields in the core and the cladding regions of optical fibers are rigorously given by the solutions of source-free Maxwell's Equations

$$\nabla \times \vec{E} = -j \left( \frac{\mu_o}{\epsilon_o} \right)^{1/2} k_o \vec{H} \quad (2.1)$$

$$\nabla \times \vec{H} = \vec{J} + j \left( \frac{\epsilon_o}{\mu_o} \right)^{1/2} k_o \vec{E} \quad (2.2)$$

$$\nabla \cdot (n^2 \vec{E}) = 0 \quad (2.3)$$

$$\nabla \cdot \vec{H} = 0 \quad (2.4)$$

where  $\epsilon_o$  and  $\mu_o$  are the permittivity and the permeability of the free-space, respectively, and  $k_o = \omega \sqrt{\mu_o \epsilon_o}$ . The refractive index is denoted by  $n$ , and throughout this thesis, the core and the cladding refractive indices will be denoted by  $n_{co}$  and  $n_{cl}$ , respectively. In almost all fiber calculations,  $n_{cl}$  is assumed constant, and graded index fibers have a variation in  $n_{co}$  depending on application. In this work, the core index  $n_{co}$  is assumed constant; in other words, we restrict ourselves to step index fibers to simplify the analysis. However, for fibers used in communication systems, this does not bring a major restriction, since the difference between  $n_{co}$  and  $n_{cl}$  must be kept small to limit the dispersion (weakly guiding fibers).



The idea of the volume equivalent current method is to replace an inhomogeneous medium with a homogeneous medium having a volume current distribution. For an inhomogeneous medium, the field pattern is shaped by the inhomogeneity of the medium, whereas in the homogeneous case, by the source distribution. The equivalent current distribution yields the same field value at every point in space as the source-free inhomogeneous medium.

To obtain the volume equivalent currents, write Eq.(2.2) in core and cladding regions as follows

$$\nabla \times \vec{H} = jY_o k_o n_{cl}^2 \vec{E} \quad , \quad r > \rho \quad (2.5)$$

$$\nabla \times \vec{H} = jY_o k_o n_{co}^2 \vec{E} \quad , \quad r < \rho \quad (2.6)$$

where  $Y_o = \sqrt{\epsilon_o/\mu_o}$  and  $\rho$  is the core radius.

In order to have a homogeneous medium as the equivalent current method offers, we should remove the core, leaving a volume current distribution. This procedure is equal to manipulating Eq.(2.6) as follows

$$\nabla \times \vec{H} = jY_o k_o n_{co}^2 \vec{E} - jY_o k_o n_{cl}^2 \vec{E} + jY_o k_o n_{cl}^2 \vec{E} \quad (2.7)$$

$$= \vec{J}_{eq} + jY_o k_o n_{cl}^2 \vec{E} \quad (2.8)$$

where

$$\vec{J}_{eq} = jY_o k_o (n_{co}^2 - n_{cl}^2) \vec{E} \quad (2.9)$$

is the equivalent current. If  $\vec{E}$  is known or approximated, then the radiation can be calculated by using antenna theory as described briefly below.

From Eq.(2.4) one can deduce that there exists a vector  $\vec{A}$  called the magnetic vector potential, such that

$$\vec{H} = \frac{1}{\mu_o} \nabla \times \vec{A} \quad (2.10)$$

We can manipulate the Maxwell's equations to get

$$\vec{E} = \frac{-jk_o}{(\mu_o \epsilon_o)^{1/2}} \left\{ \vec{A} + \frac{1}{k_o^2 n^2} \nabla(\nabla \cdot \vec{A}) \right\} \quad (2.11)$$

where  $\vec{A}$  satisfies

$$\{\nabla^2 + k_o^2 n^2\} \vec{A} = -\mu_o \vec{J}_{eq} \quad (2.12)$$

The total radiated power  $P_{rad}$ , is related to  $\vec{A}$  as follows

$$P_{rad} = \frac{c^2 k_o^2 n_{cl}}{2} \left( \frac{\epsilon_o}{\mu_o} \right)^{1/2} \int_0^\pi \int_0^{2\pi} |\hat{\mathbf{a}}_r \times \vec{A}|^2 r^2 \sin^2 \theta d\theta d\phi \quad (2.13)$$

where  $c$  is the speed of light,  $r$  is the radial distance ( $r \rightarrow \infty$ ), and  $\hat{\mathbf{a}}_r$  is the unit vector along  $r$ .

The solution of Eq.(2.12) is given as

$$\vec{A} = \frac{\mu_o}{4\pi r} \vec{M} e^{-jk_o n_{cl} r} \quad (2.14)$$

$$\vec{M} = \int_v \vec{J}_{eq}(\vec{r}') e^{jk_o n_{cl} r' \cos \gamma} d\tau' \quad (2.15)$$

where  $r'$ , and  $r$  are the length from the origin to the source point and to the field point, respectively (see Fig.2.1).

We deduce from Eqs.(2.13), (2.14) and (2.15) that

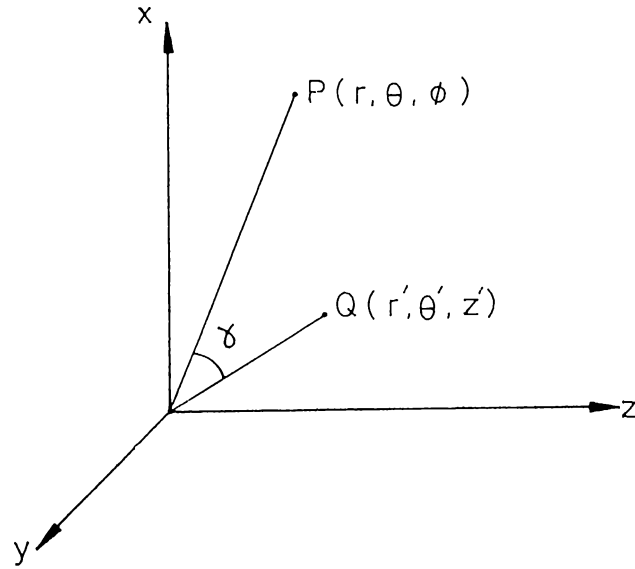


Figure 2.1: Coordinate of the source and the field points

$$P_{rad} = \frac{k_o^2 n_{cl}}{32\pi^2} \left( \frac{\mu_o}{\epsilon_o} \right)^{1/2} \int_0^{2\pi} \int_0^\pi \{ |M_\theta|^2 + |M_\phi|^2 \} \sin \theta \, d\theta \, d\phi \quad (2.16)$$

where  $M_\theta$  and  $M_\phi$  are the components of  $\vec{M}$  in spherical coordinates, and  $\hat{a}_\theta$  and  $\hat{a}_\phi$  are the unit vectors parallel to the  $\theta$ - and  $\phi$ -axis, respectively. That is

$$M_\theta = \int_{v'} \vec{J}_{eq}(r') \cdot \hat{a}_\theta e^{jkn_{cl}r' \cos \gamma} \, dr' \quad (2.17)$$

$$M_\phi = \int_{v'} \vec{J}_{eq}(r') \cdot \hat{a}_\phi e^{jkn_{cl}r' \cos \gamma} \, dr' \quad (2.18)$$

where  $v'$  is the source region, and  $\gamma$  is defined in Fig. 2.1.

Now, we are able to find the total power radiated from any current distribution. First to find  $\vec{M}$  using Eq.(2.15), and then the radiated power using Eq.(2.16).

## Chapter 3

# ANALYSIS OF DIELECTRIC OPTICAL WAVEGUIDES

It is known that many propagating modes may exist in a metallic waveguide. At a metallic boundary of a microwave guide, the continuity relationships of the tangential  $\vec{E}$  and  $\vec{H}$  fields favor the existence of only the *transverse electric*, *TE*, or the *transverse magnetic*, *TM*, modes along the guide. No fields can exist outside the guide. In the dielectric waveguide, the situation is more complex due to the boundary condition. All six components (3 for  $\vec{E}$ , and 3 for  $\vec{H}$ ) can coexist for one mode. Those modes with strong  $E_z$  field compared to  $H_z$  are designated as *EH* modes. Likewise, those with a stronger  $H_z$  are called *HE* modes. Occasionally, some TE and TM modes can also exist in cylindrical and planar dielectric waveguides. In addition to the propagating modes, there are unwanted *radiation* and *evanescent modes*. The *propagating modes* are associated with discrete eigenvalues. So, they can be indexed as metallic waveguide modes.

### 3.1 FIELDS OF PLANAR WAVEGUIDES

The step-profile planar waveguide has a core of uniform refractive index  $n_{co}$  surrounded by the cladding of uniform refractive index  $n_{cl}$  (see Fig.3.1). The cladding is assumed to be unbounded. This assumption introduces only very little error,

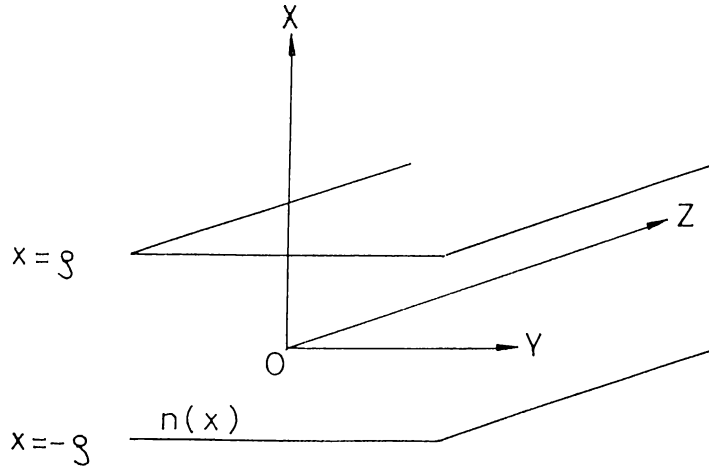


Figure 3.1: Section of a step-profile planar waveguide which is unbounded in the  $y$  and  $z$  directions. The core halfwidth is  $\rho$ , and  $n(x)$  is the refractive index profile

but simplifies the analysis considerably. The profile is described as follows

$$n(x) = \begin{cases} n_{co} & 0 \leq |x| < \rho \\ n_{cl} & \rho \leq |x| \end{cases} \quad (3.1)$$

where  $\rho$  is the core half-width.

The total field in the waveguide can be thought of as the sum of modes propagating along  $z$ -axis, and each having different propagation constant  $\beta$  as follows

$$\vec{E}(x, y, z) = \vec{E}_o(x, y)e^{-j\beta z} \quad (3.2)$$

$$\vec{H}(x, y, z) = \vec{H}_o(x, y)e^{-j\beta z} \quad (3.3)$$

Further, we can decompose those fields into two components, one parallel to

and the other orthogonal to the propagation axis, and call them *longitudinal* and *transversal* components, respectively. Then we get

$$\vec{E}(x, y, z) = (\vec{E}_{ot} + E_{oz}\hat{a}_z)e^{-j\beta z} \quad (3.4)$$

$$\vec{H}(x, y, z) = (\vec{H}_{ot} + H_{oz}\hat{a}_z)e^{-j\beta z} \quad (3.5)$$

where the subscript *oz* and *ot* are for the longitudinal and the transversal components, respectively. The above representation of the fields satisfies the homogeneous vector wave equations

$$\{\nabla_t^2 + n^2k_o^2 - \beta^2\} E_o = -(\nabla_t - j\beta\hat{a}_z)E_{ot} \cdot \nabla_t \ln n^2 \quad (3.6)$$

$$\{\nabla_t^2 + n^2k_o^2 - \beta^2\} H_o = \{(\nabla_t - j\beta\hat{a}_z) \times H_o\} \times \nabla_t \ln n^2 \quad (3.7)$$

where the two dimensional operator  $\nabla_t$  is as defined in Appendix A.

All terms involving  $\nabla_t \ln n^2$  in Eqs.(3.6), and (3.7) vanish within the core and the cladding, and for the weakly guiding case, the cladding and core indices are very close to each other i.e.  $n_{cl} \approx n_{co}$  so that those terms drop out. This yields the following scalar wave equation for the longitudinal components of  $\vec{E}$ , and  $\vec{H}$

$$\{\nabla_t^2 + n^2k_o^2 - \beta^2\} \psi = 0 \quad (3.8)$$

then it is possible to find the transverse components using the longitudinal components,  $\psi$ .

Substituting Eq.(3.1) into the above equation, and referring to Appendix A for the vector operators, we get

$$\rho^2 \left\{ \frac{d^2}{dx^2} + U^2 \right\} \psi = 0 \quad \text{for } 0 \leq |x| < \rho \quad (3.9)$$

$$\rho^2 \left\{ \frac{d^2}{dx^2} - W^2 \right\} \psi = 0 \quad \text{for } \rho \leq |x| \quad (3.10)$$

where  $U$  and  $W$  are the core and the cladding modal parameters defined as

$$U = \rho(k_o^2 n_{co}^2 - \beta^2)^{1/2} \quad (3.11)$$

$$W = \rho(\beta^2 - k_o^2 n_{cl}^2)^{1/2} \quad (3.12)$$

Solutions which are bounded everywhere vary as  $\sin(Ux/\rho)$  or  $\cos(Ux/\rho)$  in the core and as  $\exp(-W|x|/\rho)$  in the cladding.

The next step is to obtain transverse components, and apply the continuity of tangential  $\vec{E}$  and  $\vec{H}$  at  $x = \pm\rho$ , which lead to the eigenvalue equations

$$W = U \tan U \quad (3.13)$$

$$W = -\tan U \quad (3.14)$$

$$n_{co}^2 W = n_{cl}^2 U \tan U \quad (3.15)$$

$$n_{co}^2 W = -n_{cl}^2 U \cot U \quad (3.16)$$

for the even TE, odd TE, even TM, and odd TM modes, respectively.

Further manipulations yield the field components for step-profile, planar waveguide. Here, we will give only the electric field components for even TE modes to give an idea about the field distribution in slab waveguide. The complete set of modal field components both for TE and TM modes for the step-profile planar waveguide are given in Table 12-1 of [13].

$$E_{oy} = \begin{cases} \cos(\frac{Ux}{\rho}) / \cos(U) & 0 \leq |x| < \rho \\ e^{-W|x|/\rho} / e^W & \rho \leq |x| \end{cases} \quad (3.17)$$

where  $U$ ,  $W$  are found using the eigenvalue equation, and each solution represents a mode.

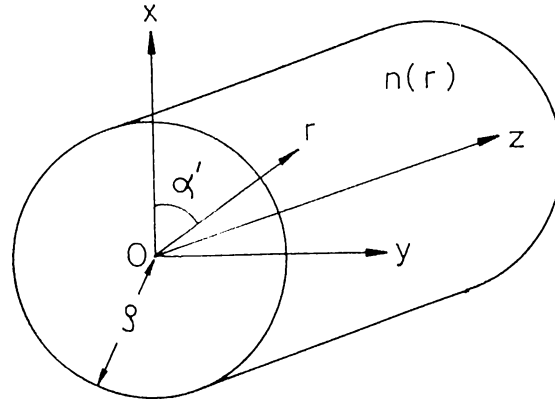


Figure 3.2: Section of a step-profile circular waveguide

### 3.2 FIELDS OF CIRCULAR WAVEGUIDES (FIBERS)

The refractive index profile of the circular waveguide is assumed as follows

$$n(r) = \begin{cases} n_{co} & 0 \leq r < \rho \\ n_{cl} & \rho \leq r \end{cases} \quad (3.18)$$

where  $\rho$  is the core radius (see Fig. 3.2).

We will decompose those fields into two components, one parallel to and the other orthogonal to the propagation axis and again call them the longitudinal and the transversal components, respectively. Then

$$\vec{E}(x, y, z) = (\vec{E}_{ot} + E_{oz}\hat{a}_z)e^{-j\beta z} \quad (3.19)$$



$$\vec{H}(x, y, z) = (\vec{H}_{ot} + H_{oz}\hat{\mathbf{a}}_z)e^{-j\beta z} \quad (3.20)$$

where the subscript *oz*, and *ot* are for the longitudinal, and transversal components, respectively.

If we substitute the field representation of Eqs.(3.19), and (3.20) into Maxwell's equations, and express  $\vec{E}_{ot}$ , and  $\vec{H}_{ot}$  in terms of  $E_{oz}\hat{\mathbf{a}}_z$ , and  $H_{oz}\hat{\mathbf{a}}_z$ , we obtain the coupled equations for the longitudinal field components

$$\begin{aligned} \{\nabla_t^2 + p\} E_{oz} - \frac{\beta^2}{p} \nabla_t E_{oz} \cdot \nabla_t \ln n^2 \\ = - \left( \frac{\mu_o}{\epsilon_o} \right)^{1/2} \frac{k_o \beta}{p} \hat{\mathbf{a}}_z \cdot (\nabla_t H_{oz} \times \nabla_t \ln n^2) \end{aligned} \quad (3.21)$$

$$\begin{aligned} \{\nabla_t^2 + p\} H_{oz} - \frac{n^2 k_o^2}{p} \nabla_t H_{oz} \cdot \nabla_t \ln n^2 \\ = \left( \frac{\mu_o}{\epsilon_o} \right)^{1/2} \frac{k_o n^2 \beta}{p} \hat{\mathbf{a}}_z \cdot (\nabla_t E_{oz} \times \nabla_t \ln n^2) \end{aligned} \quad (3.22)$$

where

$$p = k_o^2 n^2 - \beta^2 \quad (3.23)$$

As is well known for metallic circular waveguides, there exist two independent solutions, one with  $E_{oz} = 0$  everywhere and the other  $H_{oz} = 0$  everywhere. As it is mentioned before, those solutions are called the transverse electric (TE), and the transverse magnetic (TM), respectively. However, the  $\nabla_t \ln n^2$  terms are to be kept nonzero if  $n_{co}$  is not close enough to  $n_{cl}$ , and so the Eqs.(3.21), and (3.22) relate  $E_{oz}$ , and  $H_{oz}$  so that we cannot have decoupled equations like we had in the metallic circular waveguide case. Also, the modes of the dielectric cylindrical waveguides are in general hybrid modes, that each mode has both nonzero  $E_{oz}$ , and  $H_{oz}$  terms since the boundary conditions cannot be satisfied by taking  $E_{oz} = 0$  solution nor by taking  $H_{oz} = 0$  solution individually.

To satisfy the boundary conditions at  $r = \rho$ , we choose the longitudinal components as

$$E_{oz} = \begin{cases} A \frac{J_\nu(UR)}{J_\nu(U)} \begin{Bmatrix} \cos(\nu\phi) \\ \sin(\nu\phi) \end{Bmatrix} & 0 \leq R < 1 \\ A \frac{K_\nu(WR)}{K_\nu(W)} \begin{Bmatrix} \cos(\nu\phi) \\ \sin(\nu\phi) \end{Bmatrix} & 1 \leq R \end{cases} \quad (3.24)$$

and

$$H_{oz} = \begin{cases} B \frac{J_\nu(UR)}{J_\nu(U)} \begin{Bmatrix} -\sin(\nu\phi) \\ \cos(\nu\phi) \end{Bmatrix} & 0 \leq R < 1 \\ B \frac{K_\nu(WR)}{K_\nu(W)} \begin{Bmatrix} -\sin(\nu\phi) \\ \cos(\nu\phi) \end{Bmatrix} & 1 \leq R \end{cases} \quad (3.25)$$

where A and B are constants,  $R = r/\rho$ ,  $\nu$  is a positive integer or zero,  $J_\nu$  and  $K_\nu$ , defined in Appendix B, are the Bessel function of the first kind and the modified Bessel function of the second kind, respectively, and the upper term in the curly brackets denotes the even mode where the lower term denotes the odd mode.

The transverse components can be found using the longitudinal components. The complete set of modal field components both for TE and TM modes for step-profile circular waveguide are given in Table 12-3 of [13]. Imposing the continuity of the azimuthal components  $E_{o\phi}$  and  $H_{o\phi}$  at  $R = 1$ , we get two independent equations. Using these two equations we obtain the ratio  $A/B$  and the eigenvalue equation of EH and HE modes for step-profile fiber. Those expressions are given in the Appendix C.

### 3.3 FIELDS OF WEAKLY GUIDING FIBERS

The difference between the refractive indices of the core and the cladding regions must be very small (less than 1%) in practical fibers used in communications to keep the pulse dispersion small. These fibers are called *weakly guiding fibers*. In a weakly guiding fiber, the index difference parameter  $\Delta$ , defined as

$\Delta = (n_{co}^2 - n_{cl}^2)/2n_{co}^2$ , is small. Gloge [14], and Snyder et.al. [15] has shown that in weakly guiding case, the combinations of hybrid modes have the field pattern resembling a linearly polarized structure at least for the lower order modes. Those modes are named *linearly polarized LP<sub>vm</sub> modes*, the fundamental  $HE_{11}$  mode is named the  $LP_{01}$  mode, the  $TE_{01}$ ,  $TM_{01}$  and  $HE_{21}$  combination mode as the  $LP_{11}$  mode, etc. Due to relative simplicity of this notation, it has been universally accepted for mode designation of small  $\Delta$  fiber.

To determine the expressions for  $LP$  modes, we will again decompose the fields into the transverse and the longitudinal components.

$$\vec{E}(x, y, z) = \vec{E}_o(x, y)e^{-j\beta z} \quad (3.26)$$

$$= (\vec{E}_{ot} + E_{oz}\hat{a}_z)e^{-j\beta z} \quad (3.27)$$

$$\vec{H}(x, y, z) = \vec{H}_o(x, y)e^{-j\beta z} \quad (3.28)$$

$$= (\vec{H}_{ot} + H_{oz}\hat{a}_z)e^{-j\beta z} \quad (3.29)$$

The transverse components of  $LP$  modes can be written as (transverse electric field is chosen in  $y$  direction)

$$E_y = H_x \begin{cases} Z_o/n_{co} & 0 \leq R < 1 \\ Z_o/n_{cl} & 1 \leq R \end{cases} \quad (3.30)$$

$$= E_v \begin{cases} \frac{J_v(UR)}{J_v(U)} \begin{Bmatrix} \cos(v\phi) \\ \sin(v\phi) \end{Bmatrix} & 0 \leq R < 1 \\ \frac{K_v(WR)}{K_v(W)} \begin{Bmatrix} \cos(v\phi) \\ \sin(v\phi) \end{Bmatrix} & 1 \leq R \end{cases} \quad (3.31)$$

where  $Z_o = Y_o^{-1}$  is the impedance of the free space,  $E_v$  is the electric field strength at the core-cladding boundary.

The longitudinal components can be obtained from the following equations

$$E_z = -\frac{jZ_o}{k_o} \frac{\partial H_x}{\partial y} \begin{cases} 1/n_{co}^2 & 0 \leq R < 1 \\ 1/n_{cl}^2 & 1 \leq R \end{cases} \quad (3.32)$$

$$H_z = -\frac{j}{k_o Z_o} \frac{\partial E_y}{\partial x} \quad (3.33)$$

This yields

$$E_z = \frac{jE_v}{2k_o \rho} \left\{ \begin{array}{l} \frac{U}{n_{co}} \frac{J_{v+1}(UR)}{J_v(U)} \sin(v+1)\phi + \frac{U}{n_{co}} \frac{J_{v-1}(UR)}{J_v(U)} \sin(v-1)\phi \\ \frac{W}{n_{cl}} \frac{K_{v+1}(WR)}{K_v(W)} \sin(v+1)\phi - \frac{W}{n_{co}} \frac{K_{v-1}(WR)}{K_v(W)} \sin(v-1)\phi \end{array} \right\} \quad (3.34)$$

$$H_z = \frac{jE_v}{2k_o Z_o \rho} \left\{ \begin{array}{l} U \frac{J_{v+1}(UR)}{J_v(U)} \cos(v+1)\phi - U \frac{J_{v-1}(UR)}{J_v(U)} \cos(v-1)\phi \\ W \frac{K_{v+1}(WR)}{K_v(W)} \cos(v+1)\phi + W \frac{K_{v-1}(WR)}{K_v(W)} \cos(v-1)\phi \end{array} \right\} \quad (3.35)$$

The previous field values in Eq.(3.31) can be written [14] in cylindrical coordinates to match the fields at the interface. We then have

$$E_\phi = \frac{E_v}{2} (\cos(v+1)\phi + \cos(v-1)\phi) \begin{cases} \frac{J_v(UR)}{J_v(U)} & 0 \leq R < 1 \\ \frac{K_v(WR)}{K_v(W)} & 1 \leq R \end{cases} \quad (3.36)$$

$$H_\phi = -\frac{E_v}{2Z_o} (\sin(v+1)\phi - \sin(v-1)\phi) \begin{cases} n_{co} \frac{J_v(UR)}{J_v(U)} & 0 \leq R < 1 \\ n_{cl} \frac{K_v(WR)}{K_v(W)} & 1 \leq R \end{cases} \quad (3.37)$$

The boundary conditions on the core-cladding interface yields the following eigenvalue equation for the linearly polarized  $LP_{vm}$  modes.

$$U \left( \frac{J_{v-1}(U)}{J_v(U)} \right) = \pm W \left( \frac{K_{v-1}(W)}{K_v} \right) \quad (3.38)$$

If we did the above analysis taking the transverse electric field in  $x$  direction, we would get the same eigenvalue equation. So, there are two orthogonal polarizations of the same mode. This is true for all  $LP$  modes, namely each  $LP_{vm}$  mode has two orthogonal polarizations (*degeneracy*). They have the same propagation constant, and they occur simultaneously.

Even though the eigenvalue equation for the  $LP_{vm}$  are obtained from the continuity of the axial field components, these axial components are small compared to the transverse components for the weakly guiding case. So in practice all  $LP_{vm}$  modes are taken as  $TEM$  modes with no axial components, but with different propagation constants.

## Chapter 4

### LOSS IN BENT FIBERS

It is well understood that a bent fiber radiates energy. It has been assumed that this radiation is independent of the polarization for large bend radius [10] [6]. This fact can be illustrated by the equivalent current method discussed previously. If this method is used, the problem reduces to find the radiation from an antenna in homogeneous medium. In previous works, the field is assumed to be linearly polarized in the direction perpendicular to the plane of the bend. In the following, we will analyze the loss for two orthogonal polarizations, one with polarization perpendicular to the plane of bend and the other parallel to the plane of bend. They will be called as the *perpendicular* and the *parallel polarization* cases, respectively. Since a bent fiber can be thought of as a segment of a ring, we will assume the dielectric antenna to be a closed loop of radius  $R_c$  for simplicity (see Fig. 4.1). If we denote the modal power at some reference point on the axis of the bent fiber by  $P(0)$ , the modal power at a point on the axis which is  $L$  meters away from the reference point is given as

$$P(L) = P(0)e^{-\gamma L} \quad (4.1)$$

where  $\gamma$  is called the *power attenuation coefficient*. For small power attenuation coefficient and so for large bending radius (see Appendix D for the derivation of the valid region for  $R_c/\rho$  and  $\gamma$ ), Eq.(4.1) approximately equals to

$$P(L) \cong P(0)(1 - \gamma L) \quad (4.2)$$

so the power attenuation coefficient is

$$\gamma = \frac{P(0) - P(L)}{LP(0)} \quad (4.3)$$

Then the power attenuation coefficient of a circularly bent fiber with a bend radius  $R_c$  can be found using

$$\gamma = \frac{P_{rad}}{2\pi R_c P(0)} \quad (4.4)$$

where the radiated power ( $P_{rad}$ ) is assumed to be so small that the fields of the bent fiber are approximately equal to that of the straight fiber. Obviously, this approximation gets better as the radius of curvature of the bend ( $R_c$ ) increases. To get a feeling of the validity of this approximation, we can find the value of  $R_c$  for which the radiated power is smaller than 1% of the power carried by the core. So

$$\frac{P_{rad}}{P_{co}} \leq 0.01 \quad (4.5)$$

where  $P_{co}$  is the power carried by the core and it can be derived using

$$P_{co} = \int_0^{2\pi} \int_0^\rho (\vec{\mathbf{E}} \times \vec{\mathbf{H}}) \cdot \hat{\mathbf{a}}_z r d\alpha' dr \quad (4.6)$$

where

$$\vec{\mathbf{E}} = \hat{\mathbf{a}}_y \frac{J_\nu(UR)}{J_\nu(U)} \cos(\nu\phi) \quad (4.7)$$

$$\vec{\mathbf{H}} = -\hat{\mathbf{a}}_x \frac{j}{k_o n_{co} Z_o} \frac{\partial E_y}{\partial x} \quad (4.8)$$

where  $x, y, z$  coordinates are as defined in Fig. 3.2.

Substituting Eq.(4.46) into Eq.(4.5), we get

$$\frac{\pi^{1/2}}{32} \left( \frac{R_c}{\rho} \right)^{1/2} \frac{Z_o}{P_{co}} \frac{V^2}{W^{3/2}} \frac{n_{co}}{\Delta} \exp\left( -\frac{4}{3} \frac{R_c}{\rho} \frac{\Delta W^3}{V^2} \right) \leq 0.01 \quad (4.9)$$

Then  $R_c$  satisfies

$$\left(\frac{R_c}{\rho}\right)^{1/2} \exp\left(-\frac{4 R_c \Delta W^3}{3 \rho V^2}\right) \leq \frac{0.32 P_{co} W^{3/2} \Delta}{\pi^{1/2} Z_o V^2 n_{co}} \quad (4.10)$$

and

$$\gamma < \frac{P_{rad}}{2\pi R_c P_{co}} \quad (4.11)$$

If we take  $P_{rad}/P_{co} = 0.01$  then the valid region bound for  $\gamma$  is

$$\gamma < \frac{0.01}{2\pi R_c} \quad (4.12)$$

To get a practical value for  $R_c$  and  $\gamma$  let us take

$$\begin{aligned} n_{co} &= 1.560 & \lambda_o &= 850nm \\ n_{cl} &= 1.557 & \rho &= 5\mu m \end{aligned}$$

so that

$$\begin{aligned} V &= 3.574 & U &= 1.857 \\ \Delta &= 0.006 & W &= 3.055 \end{aligned}$$

Then we get

$$\begin{aligned} R_c &\cong 0.01m \\ \gamma &= 0.16 \end{aligned}$$

So, the approximation employed here introduces very little error for bend radii down to 1cm.



## 4.1 Perpendicular Polarization Case

To find the radiation due to an equivalent current distribution (see Fig 4.2), we need the electric field only in the core region since the equivalent current is zero in the cladding. For the weakly guiding straight fiber, the electric field for each mode is given in Eq.(3.31).

If the loss is small and also the radius of the bend  $R_c$  is much larger than the core radius  $\rho$ , we can assume the field of the bent fiber to be approximately equal to the core field distribution of the straight fiber (see Appendix D), so that the field is

$$E_z = F_v(R)\cos(l\alpha')e^{-j\beta s} \quad (4.13)$$

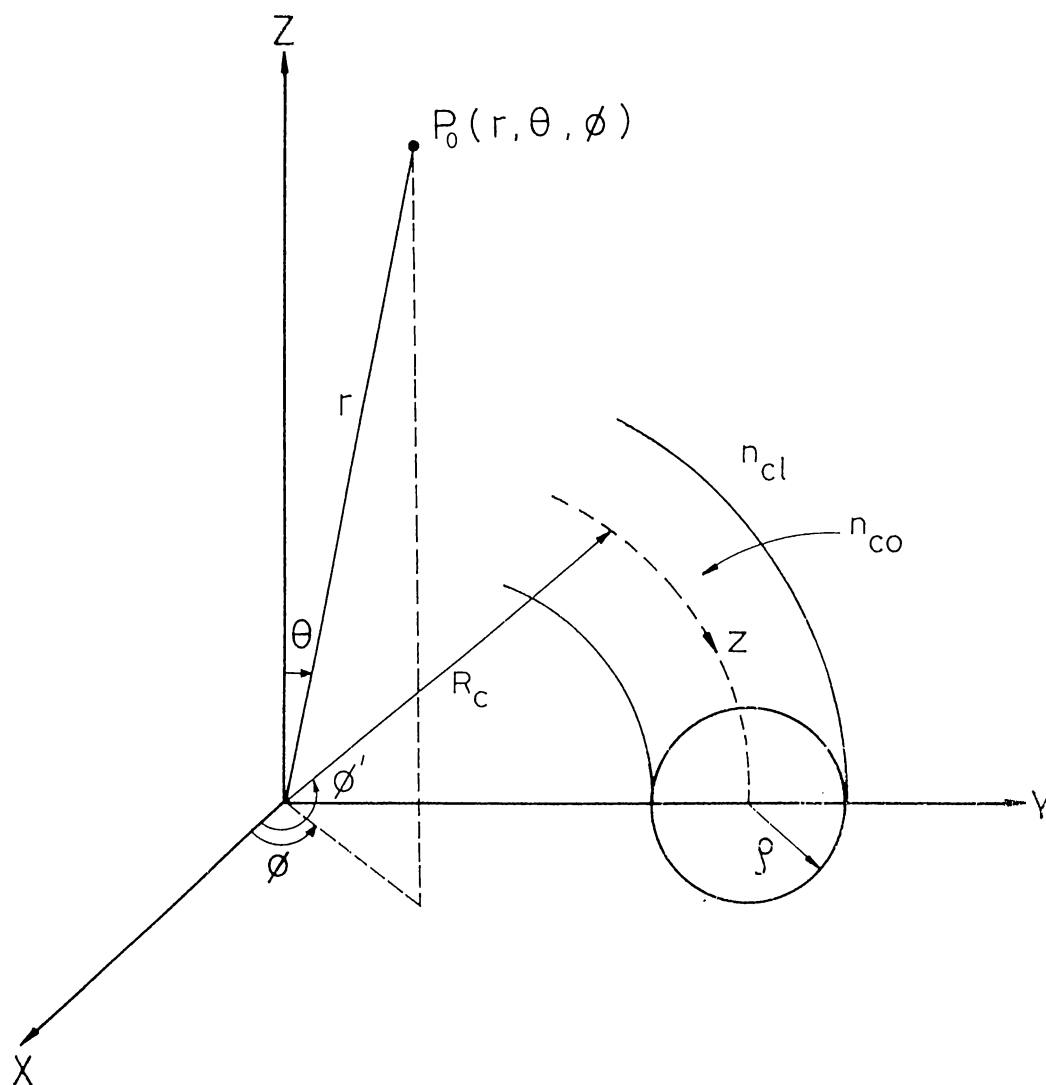
where  $s$  is the length along the fiber,  $\alpha'$  is shown in Fig. 3.2, and  $F_v(R)$  is defined as

$$F_v(R) = \frac{J_v(UR)}{J_v(U)} \quad (4.14)$$

Using the equivalent current method, and Eqs.(2.9) and (4.13) we can find the volume current distribution to be

$$\vec{J}_{eq} = jY_0k_o(n_{co}^2 - n_{cl}^2)F_v(R)\cos(l\alpha')e^{-j\beta s}\hat{a}_z \quad (4.15)$$

To find the radiation, we need to find the vector  $M$ , to substitute this value into Eq.(2.16).

Figure 4.1: *The circularly bent fiber*

$$\vec{M} = \hat{\mathbf{a}}_z \int_v J(r') e^{-jk_o n_{cl} r' \cos \gamma} dr' \quad (4.16)$$

$$= \hat{\mathbf{a}}_z \int_0^\rho \int_0^{2\pi} \int_0^\pi j Y_o k_o (n_{co}^2 - n_{cl}^2) F_v(R) \cos(l\alpha') \cdot e^{-j\beta R_c \phi' + j k_o n_{cl} R_c \cos \gamma} dR R_c d\phi' d\alpha' \quad (4.17)$$

where the primed and unprimed coordinates are for the source and field points (see Fig. 2.1), respectively, and the relationship  $\cos \gamma = \sin \theta \cos(\theta' - \theta)$  follows from geometry, and the integration over  $R$  is in  $[0,1]$ , because the volume current exists only in the core region. The exponent  $\exp(-j\beta R_c \phi')$  is the phase difference of the current sources due to the transmission delay, and the exponent  $\exp(j k_o n_{cl} R_c \cos \gamma)$  is the phase differences of the contributions of the sources at the field point.

Integration over  $R$  and  $\alpha'$  leads to

$$M_z = I_c R_c \int_0^{2\pi} e^{-j\beta R_c \phi' + j k_o n_{cl} R_c \sin \theta \cos(\phi' - \phi)} d\phi' \quad (4.18)$$

where

$$I_c = j Y_o k_o (n_{co}^2 - n_{cl}^2) \int_0^\rho \int_0^{2\pi} F_v(R) \cos(l\alpha') dR d\alpha' \quad (4.19)$$

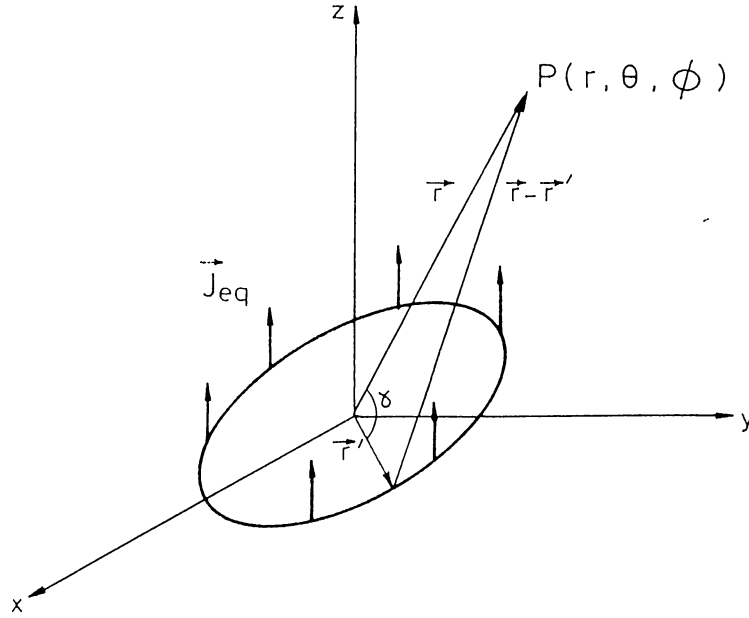
Now, we can find  $M_z$  using the definition of Bessel function

$$J_v(z) = \frac{1}{2\pi} \int_0^{2\pi} e^{-jv\phi' + jz \cos(\phi' - \phi)} d\phi' \quad (4.20)$$

to be equal to

$$\vec{M} = \hat{\mathbf{a}}_z 2\pi I_c R_c J_v(k_o n_{cl} R_c \sin \theta) \quad (4.21)$$

with  $v = \beta R_c$ .

Figure 4.2: *Circular fiber, perpendicular polarization case*

Now, the radiated power can be found by substituting Eq.(4.21) into Eq.(2.16), and this leads to [11]

$$P_{rad} = \frac{k_o^2 n_{cl}^2}{32\pi^2} Z_o \int_0^{2\pi} \int_0^\pi |M_\theta|^2 \sin \theta \, d\theta \, d\phi \quad (4.22)$$

$$= \frac{\pi}{4} k_o^2 n_{cl}^2 Z_o R_c^2 I_c^2 \int_0^\pi J_\nu(k_o n_{cl} R_c \sin \theta) \sin^3 \theta \, d\theta \quad (4.23)$$

## 4.2 Parallel Polarization Case

In this case, only the polarization of the field is different(see Fig. 4.3).

For the horizontal polarization case, the equivalent current is

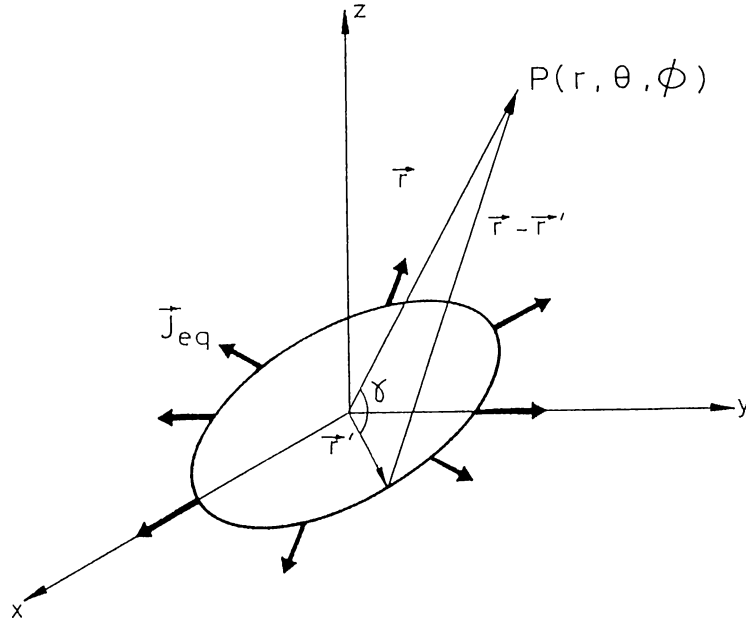


Figure 4.3: Circular fiber, parallel polarization case

$$\vec{J}_{eq} = jY_o k_o (n_{co}^2 - n_{cl}^2) F_v(R) \cos(l\alpha') e^{-j\beta s} \hat{a}_{r'} \quad (4.24)$$

where  $\hat{a}_{r'}$  is the unit vector away from the center of the curvature of the bend.

Now, in the following part, we will find  $M_\theta$  and  $M_\phi$  to substitute them into Eq.(2.16). Writing the equivalent current in cartesian coordinates

$$\vec{J}_{eq} = |\vec{J}_{eq}| \cos \phi' \hat{a}_x + |\vec{J}_{eq}| \sin \phi' \hat{a}_y \quad (4.25)$$

lead to

$$\vec{J}_{eq} \cdot \hat{a}_\theta = |\vec{J}_{eq}| (\cos \phi' \cos \phi \cos \theta + \sin \phi' \sin \phi \cos \theta) \quad (4.26)$$

$$= |\vec{J}_{eq}| \cos \theta \cos(\phi' - \phi) \quad (4.27)$$

and

$$\vec{J}_{eq} \cdot \hat{\mathbf{a}}_\phi = |\vec{J}_{eq}|(-\sin \phi \cos \phi' + \cos \phi \sin \phi') \quad (4.28)$$

$$= |\vec{J}_{eq}| \sin(\phi' - \phi) \quad (4.29)$$

So that

$$\vec{M} = \int_0^{2\pi} |\vec{J}_{eq}| R_c e^{-j\beta R_c \phi' + j k_o n_{cl} R_c \sin \theta \cos(\phi' - \phi)} (\hat{\mathbf{a}}_\theta \cos \theta \cos(\phi' - \phi) + \hat{\mathbf{a}}_\phi \sin(\phi' - \phi)) d\phi' \quad (4.30)$$

The approximate solution to the above integral can be found using the stationary phase method.

Let's find the stationary phase point(s) if exist(s).

$$\frac{\partial}{\partial \phi'} \exp(-j\beta R_c \phi' - j k_o n_{cl} R_c \sin \theta \cos(\phi' - \phi)) = 0 \quad (4.31)$$

$$\Rightarrow \sin(\phi' - \phi) = \frac{-\beta}{k n_{cl} \sin \theta} = f_1(\theta) \quad (4.32)$$

$$\Rightarrow \cos(\phi' - \phi) = \sqrt{1 - \left(\frac{\beta}{k n_{cl} \sin \theta}\right)^2} = f_2(\theta) \quad (4.33)$$

Then we have

$$\vec{M} = \int_0^{2\pi} |\vec{J}_{eq}| R_c e^{-j\beta R_c \phi' - j k_o n_{cl} R_c \sin \theta \cos(\phi' - \phi)} (\hat{\mathbf{a}}_\theta \cos \theta f_1(\theta) + \hat{\mathbf{a}}_\phi f_2(\theta)) d\phi' \quad (4.34)$$

$$= 2\pi R_c I_c J_\nu(z) \quad (4.35)$$

where  $z = k_o n_{cl} R_c \sin \theta$ .

Since  $M_\theta$  and  $M_\phi$  are known, we can find the radiated power to be in the form

$$P_{rad} = \frac{\pi}{8} k_o^2 n_{cl}^2 Z_o R_c I_c^2 \int_0^\pi \int_0^{2\pi} J_\nu^2(z) (\cos^2 \theta f_1^2(\theta) + f_2^2(\theta)) \sin \theta \, d\theta \, d\phi \quad (4.36)$$

$$= \frac{\pi}{4} k_o^2 n_{cl}^2 Z_o R_c I_c^2 \int_0^\pi J_\nu^2(z) (\cos^2 \theta f_1^2(\theta) + f_2^2(\theta)) \sin \theta \, d\theta \quad (4.37)$$

where the functions  $f_1$ , and  $f_2$  are defined in Eq.(4.32), and Eq.(4.33).

If we use Debye's approximate value for the Bessel function in the integrand, we get

$$P_{rad} = \frac{1}{8} k_o^2 n_{cl}^2 Z_o R_c I_c^2 \int_0^\pi \frac{\sin \theta Q(\theta)}{(\beta^2 - k_o^2 n_{cl}^2 \sin^2 \theta)^{1/2}} e^{S(\theta)} \, d\theta \quad (4.38)$$

where

$$S(\theta) = -\frac{2 k_o n_{cl} R_c}{3 \sin^2 \theta} \left( \frac{\beta^2}{k_o^2 n_{cl}^2} - \sin^2 \theta \right)^{3/2} \quad (4.39)$$

and

$$Q(\theta) = (\cos^2 \theta f_1^2(\theta) + f_2^2(\theta)) \quad (4.40)$$

Now, we can search for a stationary phase point of the above integral

$$\frac{\partial S(\theta)}{\partial \theta} = 0 \quad (4.41)$$

$$\Rightarrow \left( \frac{\beta^2}{k_o^2 n_{cl}^2} - \sin^2 \theta \right)^{1/2} \left( -\frac{3}{2} \sin^2 \theta - \frac{\beta^2}{k_o^2 n_{cl}^2} - \sin^2 \theta \right) = 0 \quad (4.42)$$

$$\Rightarrow \sin^2 \theta = \frac{\beta^2}{k_o^2 n_{cl}^2} \cong 1 \quad (4.43)$$

Therefore the stationary phase point is very close to  $\pi/2$ , so that  $\theta = \pi/2$  can be substituted into the coefficient function of the Bessel function in the integrand. Then we get

$$Q(\theta) = 1 \quad (4.44)$$

As a result, the radiated power for the horizontal polarization is the same as in the vertical polarization case [13].

$$P_{rad} = \frac{R_c}{8} k_o^2 n_{cl}^2 Z_o I_c^2 \int_0^\pi \frac{e^{S(\theta)}}{(\beta^2 - k_o^2 n_{cl}^2 \sin^2 \theta)^{1/2}} d\theta \quad (4.45)$$

The final expression of the radiated power is [13]

$$P_{rad} = \frac{\pi^{1/2}}{32} \left( \frac{R_c}{\rho} \right)^{1/2} Z_o \frac{V^2}{W^{3/2}} \frac{n_{co}}{\Delta} \exp \left( -\frac{4}{3} \frac{R_c}{\rho} \frac{\Delta W^3}{V^2} \right) \quad (4.46)$$

where

$$\Delta \cong \frac{n_{co} - n_{cl}}{n_{co}} \quad (4.47)$$

and  $V, W$  are the fiber and the cladding parameters respectively.

We see that the radiated powers are same for both polarizations so that we can say that the power loss of planar bends is independent of the polarization of the propagated field.

The power attenuation coefficient for both polarizations can be found [10] using the calculated powers that are radiated from the equivalent currents. That is given as follows



$$\gamma = \frac{\sqrt{\pi}}{\rho} \left( \frac{\rho}{R_c} \right)^{\frac{1}{2}} \frac{U^2}{e_v V^2 W^{3/2} K_{\nu-1}(W) K_{\nu+1}(W)} \exp \left[ -\frac{2}{3} \frac{\beta R_c}{(kn_{cl})^3} \frac{W^3}{\rho^3} \right] \quad (4.48)$$

where  $U$  is the core parameter,  $K$  is the modified Bessel function, and  $e_\nu = 2$  if  $\nu = 0$ , and  $e_\nu = 1$  otherwise.

## Chapter 5

### LOSS IN HELICAL FIBERS

In this part, we will use the same method to examine the loss mechanism due to nonplanar bends. As an example which is of practical interest, we consider a helical fiber. Helical fibers are used for measurement of high intensity currents using the Faraday rotation. In the case of helical fiber(see Fig. 5.1), the radiation is due to bending loss and helical loss [10]. If a multimode fiber is bent into a helix, the radiation acts as an effective cutoff for modes [10]. In the previous analyses, the polarization is assumed to stay parallel to a rectangular coordinate axis which is invariant with respect to the helical path. However in reality, it is well known that the polarization slips back due to the torsion of the helix [9]. So, one needs to include this rotation of polarization in the radiation calculations. Here, we perform this analysis, and observe that the total radiation is independent of the polarization slip.

The helix considered has a pitch  $P$ , and offset  $Q$  as in Fig. 5.1. The helix angle  $\theta_p$  is defined by,  $\cos \theta_p = P/(P^2 + (2\pi Q)^2)^{1/2}$ . The helix axis coincides with the  $z'$ -axis,  $\theta$ , and  $\phi$  are the spherical angles.

Let  $\alpha$  denote the speed of the rotation of polarization, then the equivalent current is given by

$$\vec{J}_{eq} = [\hat{a}_x \cos \alpha\phi' + \hat{a}_y \sin \alpha\phi']\mu \quad (5.1)$$

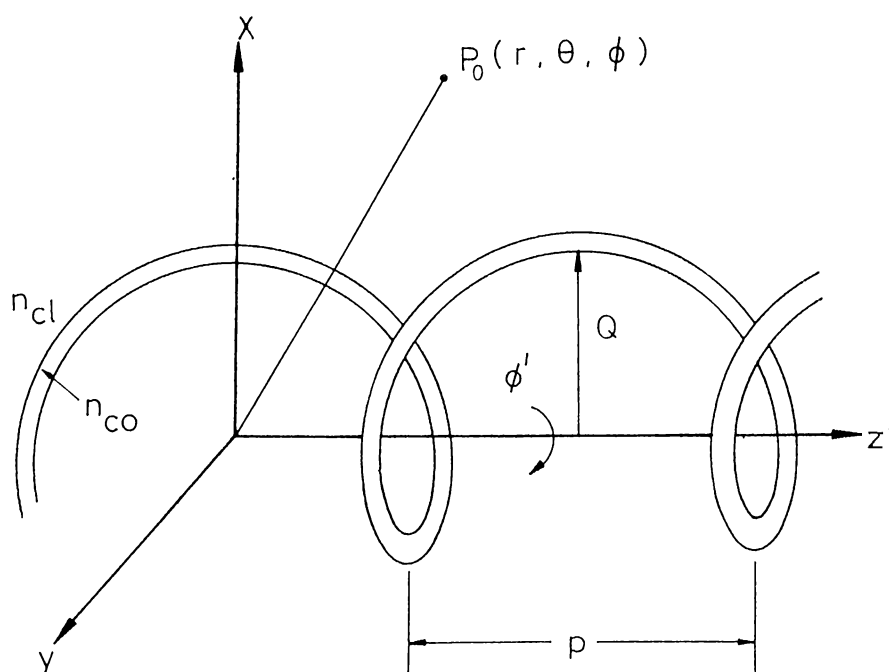


Figure 5.1: Helically bent fiber

in the core region with  $\mu$  being the magnitude of the equivalent current.

The vector potential becomes

$$\vec{M} = \hat{a}_x M_x + \hat{a}_y M_y \quad (5.2)$$

where

$$M_x = \mu \int_{-L}^L e^{-j[\frac{\beta}{\cos \theta_p} - k_{cl} \cos \theta]z' - jk_{cl}Q \sin \theta \cos(\phi - \frac{2\pi}{p}z')} \begin{Bmatrix} \cos(\alpha \frac{2\pi}{p}z') \\ \sin(\alpha \frac{2\pi}{p}z') \end{Bmatrix} dz' \quad (5.3)$$

To get the radiation from a helix of infinite length,  $L$  must be taken to infinity. Substituting

$$M_\phi = -M_x \sin \phi + M_y \cos \phi \quad (5.4)$$

$$M_\theta = M_x \cos \phi \cos \theta + M_y \sin \phi \sin \theta \quad (5.5)$$

we obtain

$$\begin{aligned} P_{rad} = & \sigma \int_0^\pi \int_0^{2\pi} [ |M_x|^2 (\sin^2 \phi + \cos^2 \phi \cos^2 \theta) \\ & + |M_y|^2 (\cos^2 \phi + \cos^2 \theta \sin^2 \phi) \\ & + |M_x| |M_y| \sin \phi \cos \phi (\cos^2 \theta - 1) ] \sin \theta \, d\theta \, d\phi \end{aligned} \quad (5.6)$$

Using the following decompositions

$$\cos\left(\alpha \frac{2\pi}{p} z'\right) = \frac{1}{2} (e^{j\alpha \frac{2\pi}{p} z'} + e^{-j\alpha \frac{2\pi}{p} z'}) \quad (5.7)$$

$$\sin\left(\alpha \frac{2\pi}{p} z'\right) = \frac{1}{2} (e^{j\alpha \frac{2\pi}{p} z'} - e^{-j\alpha \frac{2\pi}{p} z'}) \quad (5.8)$$

Eq.(5.3) can be written as

$$M_x = M_{xa} + M_{xb} \quad (5.9)$$

$$M_y = M_{ya} - M_{yb} \quad (5.10)$$

where

$$M_{x \frac{a}{b}} = \frac{\mu}{2} \int_{-L}^L e^{-j[\frac{\beta}{\cos \theta_p} - k_{cl} \cos \theta \mp \alpha \frac{2\pi}{p}]z'} e^{-jk_{cl}Q \sin \theta \cos(\phi - \frac{2\pi}{p} z')} dz' \quad (5.11)$$

and

$$M_{y \frac{a}{b}} = \frac{\mu}{2j} \int_{-L}^L e^{-j[\frac{\beta}{\cos \theta_p} - k_{cl} \cos \theta \mp \alpha \frac{2\pi}{p}]z'} e^{-jk_{cl}Q \sin \theta \cos(\phi - \frac{2\pi}{p} z')} dz' \quad (5.12)$$

Using the relation

$$e^{-jz \cos \theta} = J_0(z) + 2 \sum_{m=1}^{\infty} (j)^m J_m(z) \cos(m\theta) \quad (5.13)$$

we have

$$M_x \frac{a}{b} = \frac{\mu}{2} [J_0(k_{cl} Q \sin \theta) F_{0 \frac{a}{b}} + 2 \sum_{m=1}^{\infty} (j)^m J_m(k_{cl} Q \sin \theta) F_{m \frac{a}{b}}] \quad (5.14)$$

$$M_y \frac{a}{b} = \frac{\mu}{2j} [J_0(k_{cl} Q \sin \theta) F_{0 \frac{a}{b}} + 2 \sum_{m=1}^{\infty} (j)^m J_m(k_{cl} Q \sin \theta) F_{m \frac{a}{b}}] \quad (5.15)$$

where

$$F_m \frac{a}{b} = \int_{-L}^L e^{-j \left[ \frac{\beta}{\cos \theta_p} - k_{cl} \cos \theta \pm \alpha \frac{2\pi}{P} \right] z'} \cos \left[ m \left( \phi - \frac{2\pi}{P} z' \right) \right] dz' \quad \text{for } m \geq 0 \quad (5.16)$$

$$(5.17)$$

$$\begin{aligned} &= \frac{1}{2} e^{jm\phi} \int_{-L}^L e^{-j \left[ \frac{\beta}{\cos \theta_p} - k_{cl} \cos \theta \pm \alpha \frac{2\pi}{P} - \frac{2m\pi}{P} \right] z'} dz' \\ &+ \frac{1}{2} e^{-jm\phi} \int_{-L}^L e^{-j \left[ \frac{\beta}{\cos \theta_p} - k_{cl} \cos \theta \pm \alpha \frac{2\pi}{P} - \frac{2m\pi}{P} \right] z'} dz' \quad \text{for } m \geq 0 \end{aligned} \quad (5.18)$$

Using

$$\int_{-L}^L e^{-jaz'} dz' = 2L \frac{\sin(aL)}{aL} \quad (5.19)$$

we have

$$\begin{aligned} F_m \frac{a}{b} &= L e^{jm\phi} \frac{\sin \left[ L \left( \frac{\beta}{\cos \theta_p} - k_{cl} \cos \theta \pm \frac{\alpha 2\pi}{p} + \frac{2m\pi}{p} \right) \right]}{L \left( \frac{\beta}{\cos \theta_p} - k_{cl} \cos \theta \pm \frac{\alpha 2\pi}{p} + \frac{2m\pi}{p} \right)} \\ &+ L e^{-jm\phi} \frac{\sin \left[ L \left( \frac{\beta}{\cos \theta_p} - k_{cl} \cos \theta \pm \frac{\alpha 2\pi}{p} - \frac{2m\pi}{p} \right) \right]}{L \left( \frac{\beta}{\cos \theta_p} - k_{cl} \cos \theta \pm \frac{\alpha 2\pi}{p} - \frac{2m\pi}{p} \right)} \end{aligned} \quad (5.20)$$

Each term has a maximum at those points where the denominator is zero. Neglecting the cross terms, the square of each term has strong contribution for a discrete set of values of  $m$ .

$$|M_x|^2 = \frac{\mu^2}{4} L^2 J_o^2(k_{cl} Q \sin \theta) \left[ \frac{\sin^2[A]}{[A]^2} + \frac{\sin^2[B]}{[B]^2} \right] + \mu^2 L^2 \sum_{m=1}^{\infty} J_m^2(k_{cl} Q \sin \theta) \left[ \frac{\sin^2[C]}{[C]^2} + \frac{\sin^2[D]}{[D]^2} + \frac{\sin^2[E]}{[E]^2} + \frac{\sin^2[F]}{[F]^2} \right] \quad (5.21)$$

where

$$A = L \left( \frac{\beta}{\cos \theta_p} - k_{cl} \cos \theta - \alpha \frac{2\pi}{p} \right) \quad (5.22)$$

$$B = L \left( \frac{\beta}{\cos \theta_p} - k_{cl} \cos \theta + \alpha \frac{2\pi}{p} \right) \quad (5.23)$$

$$C = L \left( \frac{\beta}{\cos \theta_p} - k_{cl} \cos \theta - \alpha \frac{2\pi}{p} + \frac{2m\pi}{p} \right) \quad (5.24)$$

$$D = L \left( \frac{\beta}{\cos \theta_p} - k_{cl} \cos \theta + \alpha \frac{2\pi}{p} + \frac{2m\pi}{p} \right) \quad (5.25)$$

$$E = L \left( \frac{\beta}{\cos \theta_p} - k_{cl} \cos \theta - \alpha \frac{2\pi}{p} - \frac{2m\pi}{p} \right) \quad (5.26)$$

$$F = L \left( \frac{\beta}{\cos \theta_p} - k_{cl} \cos \theta + \alpha \frac{2\pi}{p} - \frac{2m\pi}{p} \right) \quad (5.27)$$

Since the speed  $\alpha$  is given by [9]

$$\alpha = \cos(\theta_p) \quad (5.28)$$

for vanishingly small fiber thickness compared with the radius of the curvature, some of the sinc functions will have peaks at imaginary values of  $\theta$ . These contributions can be neglected and  $|M_x|^2$  is written as

$$|M_x|^2 = \frac{\mu^2}{4} L^2 J_o^2(k_{cl} Q \sin \theta) \left[ \frac{\sin^2[A]}{[A]^2} \right] + \mu^2 L^2 \sum_{m=m_{\min}}^{m=m_{\max}} J_m^2(k_{cl} Q \sin \theta) \left[ \frac{\sin^2[E]}{[E]^2} + \frac{\sin^2[F]}{[F]^2} \right] \quad (5.29)$$

where  $m$  are values for which

$$\cos \theta_m = \frac{\beta}{k_{cl} \cos \theta_p} \mp \frac{\alpha 2\pi}{pk_{cl}} - \frac{2m\pi}{pk_{cl}} \quad (5.30)$$

yields a value of  $\theta_m$  between 0 and  $\pi$ . The expression for  $|M_y|^2$  is exactly the same, in other words

$$|M_y|^2 = |M_x|^2 = |M|^2 \quad (5.31)$$

Substituting these in Eq.(5.6), and noting that  $|M_x|^2$  and  $|M_y|^2$  are independent of  $\phi$  we get

$$P_{rad} = 2\pi\sigma \int_0^\pi |M|^2 (1 + \cos^2 \theta) \sin \theta \, d\theta \quad (5.32)$$

Defining

$$q_\mp = L \left( \frac{\beta}{\cos \theta_p} - k_{cl} \cos \theta \mp \frac{\alpha 2\pi}{p} - \frac{2m\pi}{p} \right) \quad (5.33)$$

$$dq_\mp = L k_{cl} \sin \theta \, d\theta \quad (5.34)$$

The integral in Eq.(5.32) becomes

$$P_{rad} = 2\pi\sigma\mu^2 L^2 \sum_m J_m^2(k_{cl}Q \sin \theta_m) (1 + \cos^2 \theta_m) \frac{1}{Lk_{cl}} \cdot \left[ \int_{z^-}^{z^+} \frac{\sin^2(q_+)}{q_+^2} dq_+ + \int_{z^-}^{z^+} \frac{\sin^2(q_-)}{q_-^2} dq_- \right] \quad (5.35)$$

where  $z^+$  and  $z^-$  correspond to the values of  $q_\pm$  when  $m$  goes from  $m_{min}$  to  $m_{max}$ . If we now increase  $L$  indefinitely, the integrals have value  $\pi$ , so

$$P_{rad} = \frac{4\pi^2\sigma\mu^2 L}{k_{cl}} \sum_m J_m^2(k_{cl}Q \sin \theta_m) (1 + \cos^2 \theta_m) \quad (5.36)$$

This expression is exactly the same as found in previous analyses (Eq.A17 of [10]) which neglected the rotation of the direction of polarization.

## Chapter 6

### CONCLUSIONS

Using the volume equivalent current method, the bending loss in a fiber is found to be independent of polarization for weakly guiding case. Any polarization can be decomposed into the weighted sum of the two orthogonal polarizations, so one can add the individual contributions to the power radiated from the two orthogonal components, thus the above result is valid for any polarization.

Similar to the previous studies, the bend radius is assumed to be very large compared to the radius of the core. This assumption simplifies the analysis considerably since by this way one can approximate the field distribution of the bent fiber by that of the straight fiber. This is equivalent to taking the radiated power small, compared to the power carried by the core. Based on this assumption, a bound on the bend radius and the attenuation constant is derived for the validity of the approximation.

Similarly the bending loss is found for a helically bent fiber. The polarization slip due to the torsion is also taken into account in the analysis. It is found that the bending loss for a helical fiber is independent of polarization even in the presence of the polarization slip.

For further work, the above results for the helically bent fiber can be generalized for multimode fiber. Also, some other practical problems can be solved, like the design of a helical coupler using the volume equivalent current method.



## Appendix A

### Scalar Operators

$$\Psi = \psi(x, y, z) \quad (\text{A.1})$$

$$\nabla_t \Psi = \hat{a}_x \frac{\partial \Psi}{\partial x} + \hat{a}_y \frac{\partial \Psi}{\partial y} \quad (\text{A.2})$$

$$= \hat{a}_r \frac{\partial \Psi}{\partial r} + \hat{a}_\phi \frac{1}{r} \frac{\partial \Psi}{\partial \phi} \quad (\text{A.3})$$

$$\nabla_t^2 \Psi = \frac{\partial^2 \Psi}{\partial x^2} + \frac{\partial^2 \Psi}{\partial y^2} \quad (\text{A.4})$$

$$= \frac{1}{r} \frac{\partial}{\partial r} \left\{ r \frac{\partial \Psi}{\partial r} \right\} + \frac{1}{r^2} \frac{\partial^2 \Psi}{\partial \phi^2} \quad (\text{A.5})$$

### Vector Operators

$$\vec{A} = A_o(x, y, z) \hat{a} \quad (\text{A.6})$$

$$\nabla_t \vec{A}_t = \frac{\partial \vec{A}_x}{\partial x} + \frac{\partial \vec{A}_y}{\partial y} \quad (\text{A.7})$$

$$= \frac{1}{r} \frac{\partial}{\partial r} (r A_r) + \frac{1}{r} \frac{\partial \vec{A}_\phi}{\partial \phi} \quad (\text{A.8})$$

$$\nabla_t \times \vec{A}_t = \hat{a}_z \left\{ \frac{\partial A_y}{\partial x} - \frac{\partial A_x}{\partial y} \right\} \quad (\text{A.9})$$

$$= \hat{a}_z \left\{ \frac{1}{r} \frac{\partial}{\partial r} (r A_\phi) - \frac{1}{r} \frac{\partial \vec{A}_r}{\partial \phi} \right\} \quad (\text{A.10})$$

## Appendix B

The Bessel function of the first kind is defined as

$$J_m(z) = \frac{1}{2\pi j^m} \int_0^{2\pi} e^{-jz \cos \theta} \cos(m\theta) d\theta \quad (\text{B.1})$$

$$= \frac{j^m}{2\pi} \int_0^{2\pi} e^{jz \cos \theta} \cos(m\theta) d\theta \quad (\text{B.2})$$

The modified Bessel function of the second kind is defined as

$$K_\nu(z) = \int_0^\infty e^{-z \cosh t} \cosh(\nu t) dt \quad (\text{B.3})$$

## Appendix C

Eigenvalue equations for step profile circular fiber, for  $HE_{\nu m}$  and  $EH_{\nu m}$  modes

$$\left\{ \frac{J'_\nu(U)}{UJ_\nu(U)} + \frac{K'_\nu(W)}{WK_\nu(W)} \right\} \left\{ \frac{J'_\nu(U)}{UJ_\nu(U)} + \frac{n_{cl}^2}{n_{co}^2} \frac{K'_\nu(W)}{WK_\nu(W)} \right\} = \left( \frac{v\beta}{kn_{co}} \right)^2 \left( \frac{V}{UW} \right)^4 \quad (C.1)$$

for  $TE_{0m}$  modes

$$\frac{J_1(U)}{UJ_0(U)} + \frac{K_1(W)}{WK_0(W)} = 0 \quad (C.2)$$

and for  $TM_{0m}$  modes

$$\frac{n_{co}^2 J_1(U)}{UJ_0(U)} + \frac{n_{cl}^2 K_1(W)}{WK_0(W)} = 0 \quad (C.3)$$

where  $m$  is the  $m$ 'th root.

## References

- [1] E. A. Marcatili, "Bends In Optical Dielectric Guides", *Bell Syst. Tech. J.* **48**, 1969, pp.2103-2132.
- [2] V. V. Shevchenko, "Radiation Losses in Bent Waveguides for Surface Waves", *Radiophys. Quantum Electron.* **14**, 1973 pp.607-614.
- [3] L. Lewin, "Radiation From Curved Dielectric Slabs and Fibers", *IEEE Trans. Microwave Tech.* MTT-**22**, 1974, pp.718-727.
- [4] A. W. Snyder, I. White, and D. J. Michell, "Radiation From Bent Optical Waveguides", *Electron. Lett.* **11**, 1975, pp.332-333.
- [5] D. Marcuse, "Bending Losses of the Asymmetric Slab Waveguide", *Bell Syst. Tech. J.* **50** 1971, pp.2551-2563.
- [6] D. Chang, E. F. Kuester, "General theory of a surface-wave propagation on a curved optical waveguide of arbitrary cross section", *IEEE J. Quantum Electron.*, 1975, QE-11 pp.903-907.
- [7] D. Marcuse, "Curvature Loss Formula For Optical Fibers", *J. Opt. Soc. Am.* **66**, No.3, March 1976, pp.216-220.
- [8] D. Marcuse, "Radiation Loss Of A Helically Deformed Optical Fiber", *J. Opt. Soc. Am.* **66**, No.10, October 1976, pp.1025-1031.
- [9] J. N. Ross, "The rotation of polarization in low birefringent monomode optical fibers due to geometrical effects", *Opt. Quantum Electron* **16**, 1984, pp.455-461.

- [10] A. Altıntaş, J. D. Love, "Effective cutoffs for modes on helical fibres", *Opt. Quantum Electron.* **22**, 1990, pp.213-226.
- [11] S. G. Tanyer, A. Altıntaş, "Optik Fiberlerde Bükülme Kayıplarının Her İki Dik Polarizasyon İçin Eşdeğer Akım Yöntemi İle Analizi", *Elektrik Mühendisliği 3. Ulusal Kongresi*, 25-30 September, İstanbul Technical University, İstanbul. pp.362-365.
- [12] A. Altıntaş, S. G. Tanyer, J. D. Love, "An Examination Of Polarization On The Radiation Losses Of Bent Optical Fibers", *Proceedings of the 1990 Bilkent International Conference on New Trends in Communication, Control, and Signal Processing*, July 1990 **1**, pp.481-487.
- [13] Allan W. Snyder, J. D. Love, *Optical Waveguide Theory*, Chapman and Hall Ltd., London, 1983.
- [14] D. Gloge, "Weakly Guiding Fibers", *Applied Optics*, Vol.10 **10**, October 1971, pp.2252-2258.
- [15] A. W. Snyder, W. R. Young, "Modes of Optical Waveguides", *J. Opt. Soc. Am.* **68**, No.3, March 1978, pp.297-309.